

# Effects of the Electron-Withdrawing Power of Substituents on the Electronic Structure and Reactivity in Oxoiron(IV) Porphyrin $\pi$ -Cation Radical Complexes

Hiroshi Fujii

Contribution from the Department of Chemistry, Faculty of Science, Hokkaido University, Sapporo 060, Japan

Received June 8, 1992

**Abstract:** The effects of the electron-withdrawing power of the substituents bound to a porphyrin ring on the electronic structures and the reactivities of oxoiron(IV) porphyrin  $\pi$ -cation radical complexes were studied by using 2,7,12,17-tetramethyl-3,8,13,18-tetraarylporphyrins (aryl = (1) mesityl, (2) 2-chloro-6-methylphenyl, (3) 2,6-dichlorophenyl, or (4) 2,4,6-trichlorophenyl) and tetrakis-5,10,15,20-tetraarylporphyrins (aryl = (5) mesityl, (6) 2-chloro-6-methylphenyl, (7) 2,6-dichlorophenyl, or (8) 2,4,6-trichlorophenyl). The electronic structures of oxoiron(IV) porphyrin  $\pi$ -cation radicals were investigated by low-temperature UV-visible absorption spectroscopy and proton NMR measurements. The absorption spectra of oxoiron(IV) porphyrin  $\pi$ -cation radicals of compounds 1-4 changed with an increase of the electron-withdrawing power of ring substituents, while those of compounds 5-8 did not. Proton NMR measurements demonstrated that oxoiron(IV) porphyrin  $\pi$ -cation radicals of compounds 1-4 have an  $a_{1u}$  radical character and that those of compounds 5-8 are better described as an  $a_{2u}$  radical species. The reactivities of oxygen atoms of oxoiron(IV) porphyrin  $\pi$ -cation radicals were examined by competitive epoxidation of cyclohexene by two oxoiron(IV) porphyrin  $\pi$ -cation radicals with different radical orbital occupancies or oxidation potentials. The oxygen atom with the higher oxidation potential was more reactive than that with the lower oxidation potential. Furthermore, the oxygen atom with the  $a_{1u}$  radical state was almost as reactive as that with the  $a_{2u}$  radical state. The results indicate that the reactivity of the oxygen atom of the oxoiron(IV) porphyrin  $\pi$ -cation radical depends on its oxidation potential and is not affected by the  $a_{1u}/a_{2u}$  orbital occupancy.

## Introduction

Oxoiron compounds are believed to participate in the biochemical cycles of several different kinds of heme enzymes by performing essential oxidations in various biochemical pathways.<sup>1-4</sup> For example, horseradish peroxidase (HRP)<sup>1</sup> and catalase (CAT),<sup>1</sup> when activated by peroxides and peracids, form an oxoiron(IV) porphyrin  $\pi$ -cation radical intermediate called compound I. Compound I is also believed to be formed in the reactions of mixed function oxygenases, such as cytochrome P-450.<sup>2</sup> In spite of the common active intermediate, the reactivities of compounds I differ from enzyme to enzyme. In cytochrome P-450, the compound I species transfers a single oxygen atom directly to a variety of substrates,<sup>5</sup> while with HRP and CAT, compound I species oxidize organic compounds and hydrogen peroxide, respectively.<sup>6</sup> These diverse compound I functions have been thought to depend on heme environmental structures, such as porphyrin peripheral structures, the heme proximal ligand, and protein structures in the immediate vicinity of the heme.

Several attempts have been made to reveal the structural and functional mechanism of the diverse functions of compounds I. A study of HRP compounds I reconstituted with various synthetic iron porphyrins showed that the absorption spectra of the compounds I may be changed by altering the porphyrin peripheral side chains.<sup>7</sup> Further, the turnover catalyzed oxidations which mimic enzymatic epoxidation and hydroxylation reactions cat-

alyzed by cytochrome P-450 also reflect the catalytic activity by the porphyrin peripheral side chains. The iron tetraarylporphyrins with electronegative substituents, such as the pentafluorophenyl group, produce remarkable yield improvements in the epoxidation and hydroxylation reactions.<sup>8</sup> While these findings suggest significant changes in the electronic structures of compounds I, it is still unclear how the porphyrin side chains produce these changes.

We report here the effects of the porphyrin peripheral structure, especially of the electron-withdrawing power of the substituents, on the electronic structure and oxygen reactivity of the model compound I complex. The effects of the substituents were studied by using meso-substituted porphyrins and pyrrole  $\beta$ -substituted porphyrins with various aryl groups, as shown in Figure 1. The low-temperature UV-visible absorption spectra and proton NMR spectra measurements showed the effects of the substituents' electron-withdrawing power on the electronic states of these model compound I complexes. In previous studies, the use of turnover catalysis for the determination of the second-order rate constant for the reaction of an alkene with the compound I intermediate was generally not possible because generation of compound I was usually rate-determining. However, by preparing model compound I complexes with various electronic structures, we succeeded in directly comparing the reactivity of the oxygen atom in the competitive epoxidation reaction of cyclohexene. The results revealed the effects of the compound I radical orbital occupancy and of redox potential on oxygen reactivity.

## Experimental Section

**Materials.** Dichloromethane was refluxed over calcium hydride for 3 h and then distilled. Methanol, *m*-chloroperoxybenzoic acid (MCPBA) and tetra-*n*-butylammonium perchlorate (TBAP) were purchased from Nacal Tesque and used without further purification. Cyclohexene was

(1) (a) Dunford, H. B.; Stillman, J. S. *Coord. Chem. Rev.* 1976, 19, 187-251. (b) Dunford, H. B. *Adv. Inorg. Biochem.* 1982, 4, 41-68.

(2) Groves, J. T. *Cytochrome P-450: Structure, Mechanism, and Biochemistry*; Ortiz de Montellano, P., Ed.; Plenum: New York, 1985; Chapter I and references therein.

(3) Ortiz de Montellano, P. R. *Acc. Chem. Res.* 1987, 20, 289-294.

(4) Poulos, T. L. *Adv. Inorg. Biochem.* 1988, 7, 1-36.

(5) Griffin, B. W.; Peterson, J. A.; Estabrook, R. W. *The Porphyrins*; Dolphin, D., Ed.; Academic Press: New York, 1979; Vol. 7, pp 333-375.

(6) Hewson, W. D.; Hager, L. P. *The Porphyrins*; Dolphin, D., Ed.; Academic Press: New York, 1979; Vol. 7, pp 295-332.

(7) DiNello, R. K.; Dolphin, D. *J. Biol. Chem.* 1981, 256, 6903-6912.

(8) Traylor, P. S.; Dolphin, D.; Traylor, T. G. *J. Chem. Soc., Chem. Commun.* 1984, 279-280.

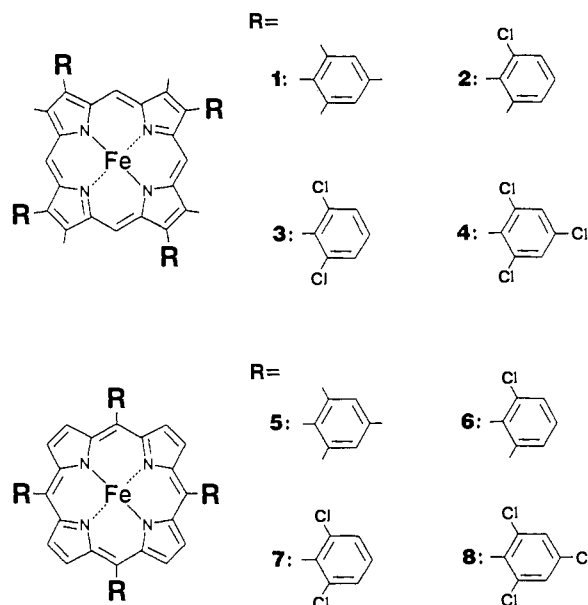


**Figure 1.** Structures of the porphyrin core of various substituted iron porphyrin complexes (1–8) employed in this study.

purchased from Wako Chemical Co. and used as received. Mesitaldehyde and 2,6-dichlorobenzaldehyde were purchased from Aldrich. 2-Chloro-6-methylbenzaldehyde was synthesized by the reduction of 2-chloro-6-methylbenzotrile with diisobutylaluminum hydride.<sup>9</sup> 2,4,6-Trichlorobenzaldehyde was prepared from 2,4,6-trichlorobenzoyl chloride.<sup>10</sup>

2,7,12,17-Tetramethyl-3,8,13,18-tetraarylporphyrins, 1–4, were synthesized by the previous method.<sup>11</sup> Absorption maxima of free bases in  $\text{CH}_2\text{Cl}_2$  were as follows [ $\lambda_{\text{max}}$  (relative intensity)]: (1) 402 (1.000), 498 (0.080), 530 (0.057), 565 (0.039), 620 (0.025); (2) 405 (1.000), 501 (0.077), 535 (0.050), 571 (0.033), 624 (0.021); (3) 407 (1.000), 502 (0.085), 536 (0.050), 572 (0.033), 625 (0.022); (4) 411 (1.000), 504 (0.080), 538 (0.049), 574 (0.035), 627 (0.023).

Iron complexes were prepared by refluxing in a chloroform–acetic acid mixture with ferrous chloride and sodium acetate. The crude iron(III) porphyrin complexes were purified by silica gel column chromatography. Absorption maxima of iron(III) chloride complexes in  $\text{CH}_2\text{Cl}_2$  were as follows [ $\lambda_{\text{max}}$  (relative intensity)]: (1) 382 (1.000), 508 (0.101), 536 (0.105), 636 (0.053); (2) 382 (1.000), 404 (0.924), 508 (0.110), 536 (0.119), 635 (0.055); (3) 383 (1.000), 407 (1.087), 508 (0.124), 537 (0.135), 635 (0.062); (4) 383 (1.000), 409 (1.109), 509 (0.145), 536 (0.152), 635 (0.073).

*meso*-Tetraarylporphyrins, 5–8, were prepared by methods described in the literature.<sup>12</sup> Absorption maxima of the free bases in  $\text{CH}_2\text{Cl}_2$  were as follows [ $\lambda_{\text{max}}$  (relative intensity)]: (5) 418 (1.000), 514 (0.040), 547 (0.012), 591 (0.011), 647 (0.006); (6) 418 (1.000), 513 (0.060), 550 (0.018), 588 (0.020), 653 (0.008); (7) 418 (1.000), 513 (0.061), 589 (0.018), 658 (0.035); (8) 424 (1.000), 513 (0.078), 556 (0.026), 588 (0.027), 658 (0.039).

Iron was inserted into the porphyrins by refluxing in acetic acid with ferrous chloride and sodium acetate. Absorption maxima of iron(III) chloride complexes in  $\text{CH}_2\text{Cl}_2$  were as follows [ $\lambda_{\text{max}}$  (relative intensity)]: (5) 377 (0.494), 418 (1.000), 510 (0.123), 578 (0.034), 655 (0.022), 693 (0.023); (6) 374 (0.445), 418 (1.000), 510 (0.112), 586 (0.037), 654 (0.027); (7) 376 (0.538), 417 (1.000), 508 (0.129), 651 (0.042); (8) 370 (0.480), 419 (1.000), 508 (0.118), 650 (0.043). Perchlorate–iron(III) porphyrin complexes of 1–8 were prepared by anion exchange by silver perchlorate.<sup>13</sup>

**Physical Measurements.** UV–visible absorption spectra were recorded on a Hitachi U-3200 spectrometer. Proton NMR spectra were recorded on a Bruker MSL-400 spectrometer. Chemical shifts were referenced

**Table I.** Half-Wave First Oxidation Potentials of Chloro Iron(III) Porphyrins<sup>a</sup>

aryl group	pyrrole $\beta$ -subst porphyrin	meso-subst porphyrin
mesityl	1, 1.08	5, 1.11
2-chloro-6-methylphenyl	2, 1.19	6, 1.29
2,6-dichlorophenyl	3, 1.22	7, 1.35
2,4,6-trichlorophenyl	4, 1.27	8, 1.45

<sup>a</sup> Potentials taken as the midpoint of reversible anodic and cathodic waves, referenced to SCE,  $\text{CH}_2\text{Cl}_2$  solvent, TBAP 0.1 M, and iron porphyrin 0.005 M.

to tetramethylsilane (TMS), and downfield shifts were given a positive sign. The concentration of samples for proton NMR spectra was 5–10 mM.

Electrochemical measurements were made with a three-electrode potentiostatic system. The working and counter electrodes were platinum wire. The reference electrode was a KCl saturated calomel electrode (SCE) separated from the bulk solution by fine glass frits. Cyclic voltammetry was measured on a HOKUTO DENKO Ltd. HA-301 potentiostat coupled with a HB-111 functional generator.

**Reaction with Cyclohexene.** The mixtures of oxoiron(IV) porphyrin  $\pi$ -cation radicals of 1 and 5, 1 and 4, and 5 and 8 were prepared by the addition of the stoichiometric amount of MCPBA to the corresponding mixtures of iron(III) porphyrin complexes at  $-80^\circ\text{C}$ . The reactions of the oxoiron(IV) porphyrin  $\pi$ -cation radicals with cyclohexene were carried out by the addition of excess (100–1000x) of cyclohexene at  $-80^\circ\text{C}$ . The reaction products were monitored by gas chromatography.

## Results

**Oxidation Potentials.** It has been reported that the first oxidation that iron(III) porphyrin complexes undergo is oxidation of the porphyrin ring.<sup>14</sup> To examine the effects of the electron-withdrawing power of the ring substituents on the orbital energy level, we performed cyclic voltammetric measurements in dichloromethane containing 0.1 M TBAP. The reversible oxidation peaks were observed in the range from 1.0 to 1.5 V vs SCE. The data for the half-wave oxidation potentials of iron(III) chloride complexes of 1–8 are listed in Table I. The oxidation potentials of iron(III) chloride complexes of 1–8 were shifted to more oxidizing potentials as the electron-withdrawing power of the substituent increased. The shift of the oxidation potential is more significant for 5–8 than for 1–4. Since these first oxidation potentials correspond to the HOMO energy level, these electrochemical measurements indicate that the HOMO energy level stabilizes with an increase in the electron-withdrawing power of the substituent.

**Absorption Spectra.** MCPBA has been shown to be a convenient stoichiometric oxidant that cleanly oxidizes iron(III) porphyrin to the oxoiron(IV) porphyrin  $\pi$ -cation radical.<sup>15</sup> We examined here the oxidation of iron(III) porphyrins of 1–8 by MCPBA in a dichloromethane–methanol mixture at  $-80^\circ\text{C}$ . The oxidation of iron(III) chloride complexes of 1–8 by MCPBA did not produce significant spectral changes, except in 5. However, the stoichiometric addition of MCPBA to iron(III) perchlorate complexes of 1–8 resulted in the formation of oxoiron(IV) porphyrin  $\pi$ -cation radicals. Figure 2 shows the absorption spectra of oxoiron(IV) porphyrin  $\pi$ -cation radicals of 1–4 in dichloromethane–methanol (5:1) at  $-80^\circ\text{C}$ . All of these spectra show characteristic porphyrin  $\pi$ -cation radical complex features: broad  $\alpha,\beta$  bands and a Soret band with decreased intensity.<sup>16</sup> The spectral features of oxoiron(IV) porphyrin  $\pi$ -cation radicals of 1–4 are changed by the substituent. As the electron-withdrawing power of the substituent increases, the Soret bands and the

(9) Paquett, L. A.; Birnberg, G. H. *J. Org. Chem.* **1975**, *40*, 1709–1713.

(10) Giles, R. G. F.; Sargent, M. V. *J. Chem. Soc., Perkin Trans. I* **1974**, 2447–2450.

(11) Ono, N.; Kawamura, H.; Bougauchi, M.; Maruyama, K. *Tetrahedron* **1990**, *46*, 7483–7496.

(12) Lindsey, J.; Wagner, R. *J. Org. Chem.* **1989**, *54*, 848–836.

(13) Reed, C. A.; Mashiko, T.; Bentley, S. P.; Kastner, M. E.; Scheidt, W. R.; Spartalian, K.; Lang, G. *J. Am. Chem. Soc.* **1979**, *101*, 2948–2958.

(14) Phillippi, M. A.; Goff, H. M. *J. Am. Chem. Soc.* **1982**, *104*, 6026–6034.

(15) (a) Groves, J. T.; Hauhalter, R. C.; Nakamura, M.; Nemo, T.; Evans, B. *J. Am. Chem. Soc.* **1981**, *103*, 2884–2886. (b) Groves, J. T.; Watanabe, Y. *J. Am. Chem. Soc.* **1988**, *110*, 8443–8452.

(16) Dolphin, D.; Mulijani, Z.; Rousseau, K.; Borg, D. C.; Fajer, J.; Felton, R. H. *Ann. N.Y. Acad. Sci.* **1973**, *206*, 177–199.

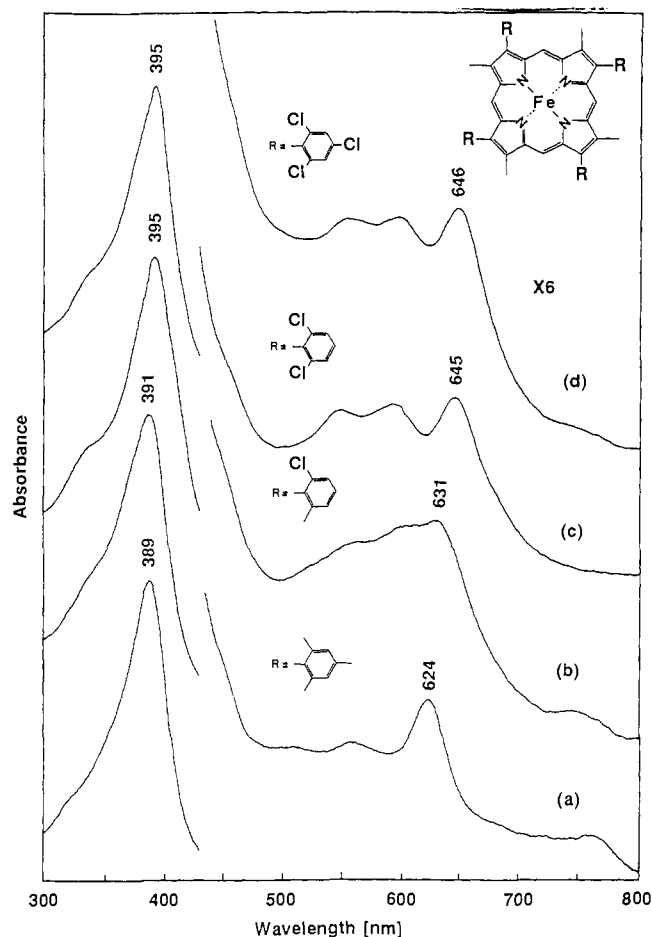


**Figure 2.** UV-visible absorption spectra of oxoiron(IV) porphyrin  $\pi$ -cation radicals of 1–4 in dichloromethane–methanol (5:1) at  $-80\text{ }^{\circ}\text{C}$ : (a) 1, (b) 2, (c) 3, (d) 4.

absorbances around 600–700 nm exhibit a red-shift, and the absorbances around 500–600 nm increase their intensities. It is interesting that the spectral features of the oxoiron(IV) porphyrin  $\pi$ -cation radical of compound 4 closely resemble those of HRP compound I.<sup>17</sup>

The absorption spectra of oxoiron(IV) porphyrin  $\pi$ -cation radicals of 5–8 are summarized in Figure 3. While an increase of the electron-withdrawing power of the substituent produces a blue-shift of the Soret bands and a red-shift of the peaks around 650 nm, the overall spectral features are generally unchanged. The spectral features of oxoiron(IV) porphyrin  $\pi$ -cation radicals of 5–8 are similar to those of CAT compound I.<sup>17</sup> UV-visible spectral data are summarized in Table II.

**NMR Spectra.** Figure 4 shows proton NMR spectra of oxoiron(IV) porphyrin  $\pi$ -cation radicals of 1–4 in dichloromethane- $d_2$ -methanol- $d_4$  (5:1) at  $-70\text{ }^{\circ}\text{C}$ . The oxoiron(IV) porphyrin  $\pi$ -cation radicals of 1–4 yielded well-resolved hyperfine-shifted proton NMR spectra that differed from those of parent iron(III) porphyrins. The signals were assigned based upon the selected deuterated samples and the intensities of the signals. The signals that showed large downfield shifts from 140 to 170 ppm were attributed to the pyrrole  $\beta$ -methyl protons, and small peaks from  $-10$  to 50 ppm were attributed to the meso proton. The pyrrole  $\beta$ -phenyl meta protons were observed in the range from 7 to 15 ppm. NMR spectral data are presented in Table II. The downfield shifts of the meso proton signals of 1 and 2 were due to the negative spin density of the meso carbon, which arises from the electron correlation effect. The small isotropic shifts of meso proton signals of 1–4 indicate the formation of an  $a_{1u}$  radical

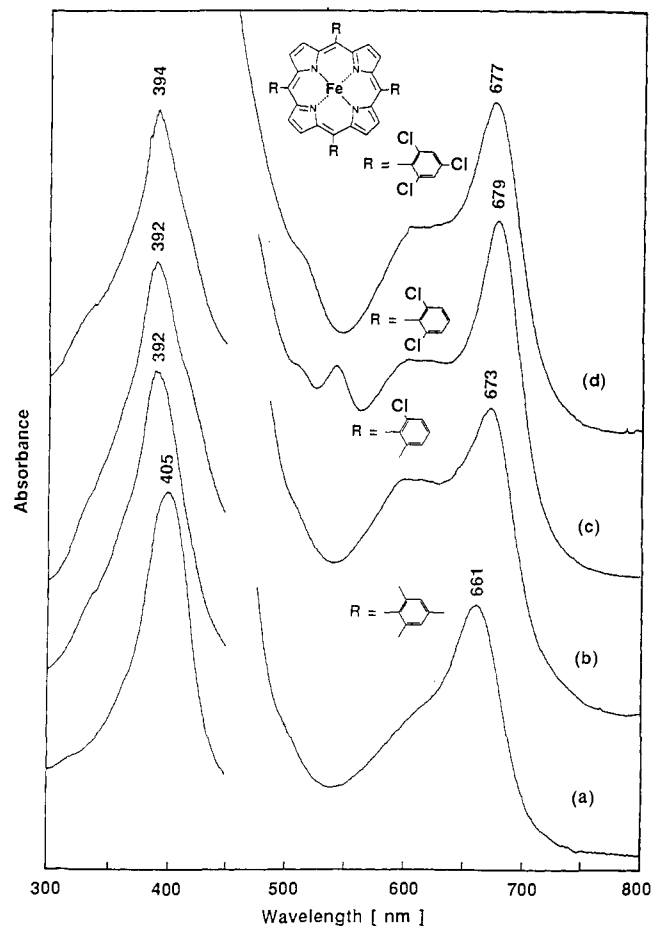


**Figure 3.** UV-visible absorption spectra of oxoiron(IV) porphyrin  $\pi$ -cation radicals of 5–8 in dichloromethane–methanol (5:1) at  $-80\text{ }^{\circ}\text{C}$ : (a) 5, (b) 6, (c) 7, (d) 8.

species. The broadening of the methyl proton signal and the split of the meso proton signal of 2 are due to the atropisomers. The splitting of meta proton signals in 1–4 is indicative of two different axial ligands, i.e., the oxygen atom and the solvent molecule. An increase of the electron-withdrawing power of the porphyrin substituent shifts the meso proton signals upfield, while the pyrrole  $\beta$ -methyl proton signals are shifted downfield.

NMR spectra of oxoiron(IV) porphyrin  $\pi$ -cation radicals of 5–8 are shown in Figure 5. Signals in the downfield region were assigned to the meta proton signals of meso aryl groups, and those in the upfield region were due to the pyrrole  $\beta$ -protons. The spectrum for 5 was identical with that in the previous report.<sup>15</sup> The separation of meta proton signals of 6 is also due to atropisomers. The proton NMR shifts for 5–8 are also compiled in Table II. As the electron-withdrawing power of the porphyrin substituent increases, the pyrrole  $\beta$ -proton and meta proton signals are shifted upfield. The large downfield shifts of the meta proton signals of 5–8 suggest the existence of a large  $\pi$ -spin density on the meso carbon, which is interpreted as an  $a_{2u}$  radical state for oxoiron(IV) porphyrin  $\pi$ -cation radicals of 5–8. As will be described in more detail in the Discussion section, the upfield shift of the pyrrole  $\beta$ -proton and the decrease of the isotropic shift of the meta proton, with an increase in the electron-withdrawing power of the substituent, are due to the contribution of an  $a_{1u}$  radical state via vibronic coupling.

Extensive variable temperature ( $-40$  to  $-80\text{ }^{\circ}\text{C}$ ) NMR measurements were made for oxoiron(IV) porphyrin  $\pi$ -cation radicals of 1–8. The results were summarized as Curie law plots. The plots for all paramagnetic signals of oxoiron(IV) porphyrin  $\pi$ -cation radicals of 1–8 were adequately linear and had intercepts near the diamagnetic region.

**Reaction with Cyclohexene.** Since we were able to characterize

(17) Dolphin, D.; Forman, A.; Borg, D. C.; Fajer, J.; Felton, R. H. *Proc. Natl. Acad. Sci. U.S.A.* 1971, 68, 614–618.

Table II. UV-Vis Absorption Spectral and Proton NMR Spectral Data of Oxoiron(IV) Porphyrin  $\pi$ -Cation Radicals<sup>a</sup>

porphyrin	UV-vis spectra (nm)	NMR spectra (ppm from TMS)		
		pyrrole $\beta$ -methyl	meso	<i>m</i> -H
1	389, 562, 624, 753	139.0	53.4	14.9, 14.0
2	391, 565, 601, 631	151.8	32.4, 30.8, 30.5, 29.1, 28.1, 27.3	12.8, 12.7, 12.6, 12.1, 12.0, 11.9, 11.8, 11.1
3	395, 551, 593, 645	164.7	-3.0	10.9, 9.8
4	395, 555, 597, 646	166.9	-7.5	10.5, 9.4
		pyrrole	<i>o</i> -methyl	<i>m</i> -H
5	405, 661	-27.6	27.2, 24.5	70.6
6	392, 673	-44.1	24.4, 21.7	55.5, 47.8, 47.7
7	392, 679	-65.5		34.8
8	394, 677	-72.7		30.0

<sup>a</sup> In dichloromethane-*d*<sub>2</sub>-methanol-*d*<sub>4</sub> (5:1) at -70 °C for 1-4 and at -80 °C for 5-8.

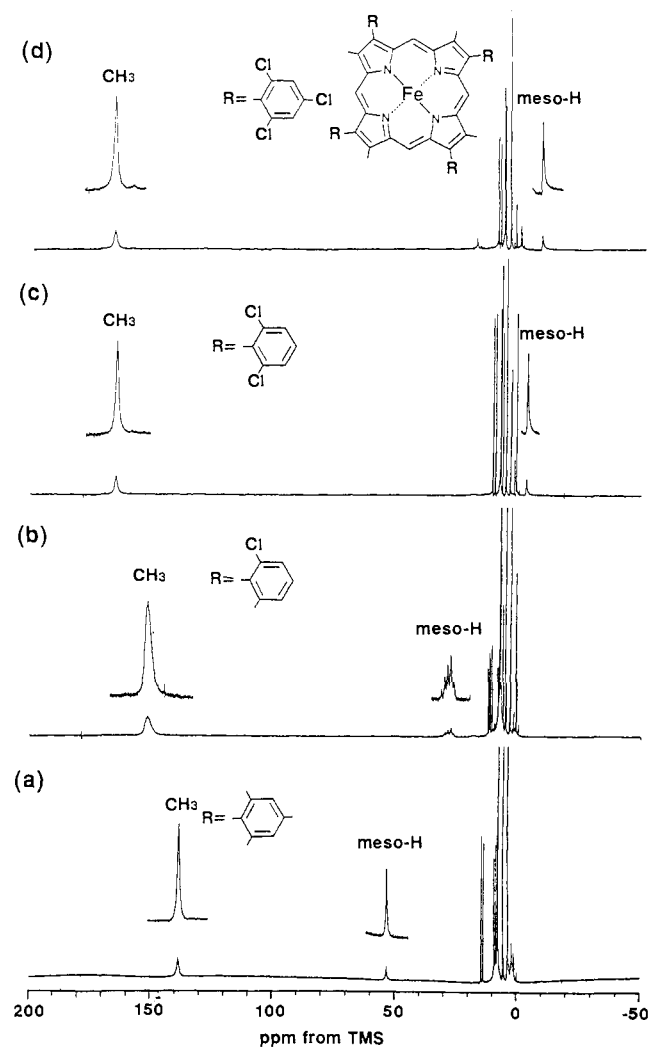


Figure 4. Proton NMR spectra of oxoiron(IV) porphyrin  $\pi$ -cation radicals of 1-4 in dichloromethane-*d*<sub>2</sub>-methanol-*d*<sub>4</sub> at -70 °C: (a) 1, (b) 2, (c) 3, (d) 4.

$a_{1u}$  and  $a_{2u}$  oxoiron(IV) porphyrin  $\pi$ -cation radicals with various oxidation potentials in the preceding section, we monitored absorption spectra to study the effects of orbital occupancy and oxidation potential of oxoiron(IV) porphyrin  $\pi$ -cation radicals on the reactivity of the oxygen atom.

The reactions of oxoiron(IV) porphyrin  $\pi$ -cation radicals of 1-8 with cyclohexene were carried out at -80 °C. Each of the oxoiron(IV) porphyrin  $\pi$ -cation radicals could react with cyclohexene. Product analysis by gas chromatography indicated the formation of cyclohexene oxide.

To compare the reactivity of the oxygen atom of an  $a_{1u}$  oxoiron(IV) porphyrin  $\pi$ -cation radical complex with that of an  $a_{2u}$  radical

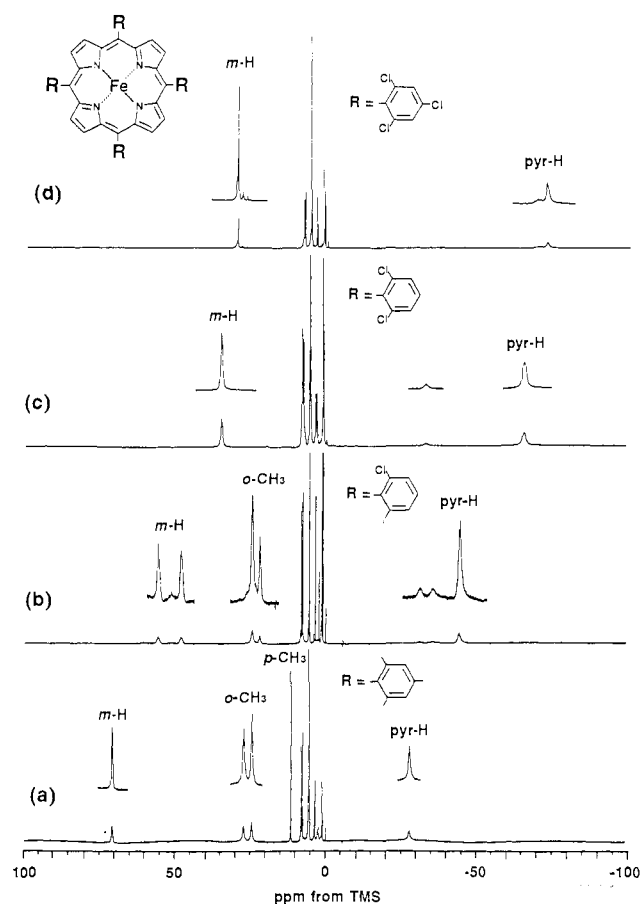
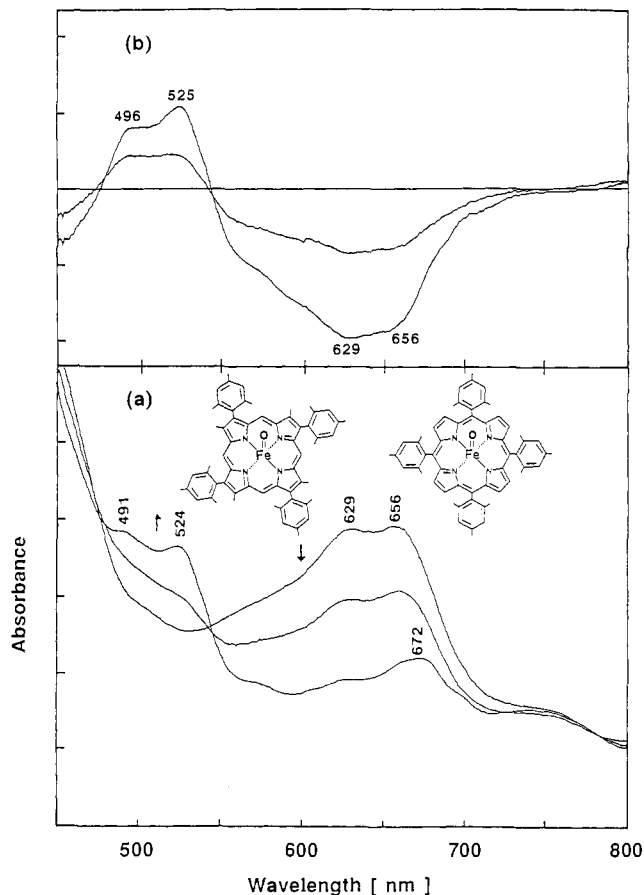


Figure 5. Proton NMR spectra of oxoiron(IV) porphyrin  $\pi$ -cation radicals of 5-8 in dichloromethane-*d*<sub>2</sub>-methanol-*d*<sub>4</sub> at -80 °C: (a) 5, (b) 6, (c) 7, (d) 8.

complex, we monitored the reaction of a mixture of oxoiron(IV) porphyrin  $\pi$ -cation radical complexes of 1 and 5 with cyclohexene. Figure 6a shows the changes in the absorption spectra of the reaction mixture after addition of cyclohexene. The initial spectrum of the mixture of 1 and 5 exhibits the absorption maxima at 629 and 656 nm, which are attributed to the absorptions from the oxoiron(IV) porphyrin  $\pi$ -cation radicals of 1 and 5, respectively. With addition of cyclohexene, the absorption near 650 nm decreases in intensity and a new absorption peak appears around 500 nm. All of these spectral changes suggest the formation of an iron(III) porphyrin complex from the reaction of an oxoiron(IV) porphyrin  $\pi$ -cation radical with cyclohexene. To clarify which complex (1 or 5) reacted with cyclohexene, the difference spectra of Figure 6a are illustrated in Figure 6b. It is clear that the absorptions at 629 and 656 nm decrease in intensity at almost the same rate. This means that the oxygen atoms of oxoiron(IV) porphyrin  $\pi$ -cation radicals of 1 and 5 have almost



**Figure 6.** (a) Absorption spectral changes of oxoiron(IV) porphyrin  $\pi$ -cation radicals of compounds **1** and **5** for the addition of an excess amount of cyclohexene. (b) Difference absorption spectra on the basis of the initial spectrum.

the same reactivity toward cyclohexene. Therefore, the orbital occupancy of oxoiron(IV) porphyrin  $\pi$ -cation radical does not appear to affect the reactivity of the oxygen atom.

We also investigated the effect of the oxidation potential on the reactivity of oxygen atoms of oxoiron(IV) porphyrin  $\pi$ -cation radicals. The competitive reactions of the mixtures of oxoiron(IV) porphyrin  $\pi$ -cation radical complexes of **5** and **8**, and **1** and **4** with cyclohexene were examined by monitoring absorption spectra. The absorption spectra changes of the mixture of **5** and **8**, after addition of cyclohexene, are illustrated in Figure 7a. The absorption spectrum of the mixture of **5** and **8** shows an absorption maximum at 671 nm. Upon addition of cyclohexene, the absorption spectrum developed clear isosbestic points. The reaction with cyclohexene resulted in a loss of the absorption peak at 671 nm and an appearance of an absorption around 500 nm. Figure 7b shows the difference spectra of Figure 7a. The decreased peaks at 606 and 679 nm and the increased peak at 500 nm were identical with the absorbances of oxoiron(IV) porphyrin  $\pi$ -cation radical and iron(III) porphyrin of **8**, respectively. These results clearly indicate that the complex of **8** reacted with cyclohexene, and the complex with **5**, which had a lower oxidation potential, did not.

Figure 8a shows the changes in the absorption spectra of the mixture of oxoiron(IV) porphyrin  $\pi$ -cation radicals of **1** and **4**, following the addition of cyclohexene. Upon addition of cyclohexene, the absorption spectrum developed clear isosbestic points. The reaction with cyclohexene resulted in a loss of the absorption peak at 624 nm and the appearance of a new peak near 500 nm, as shown in Figure 8a. The difference spectra of Figure 8b show the decreases of the peaks at 597 and 647 nm and the increase of the absorbance near 500 nm. These were easily recognized as the respective peaks of oxoiron(IV) porphyrin  $\pi$ -cation radical

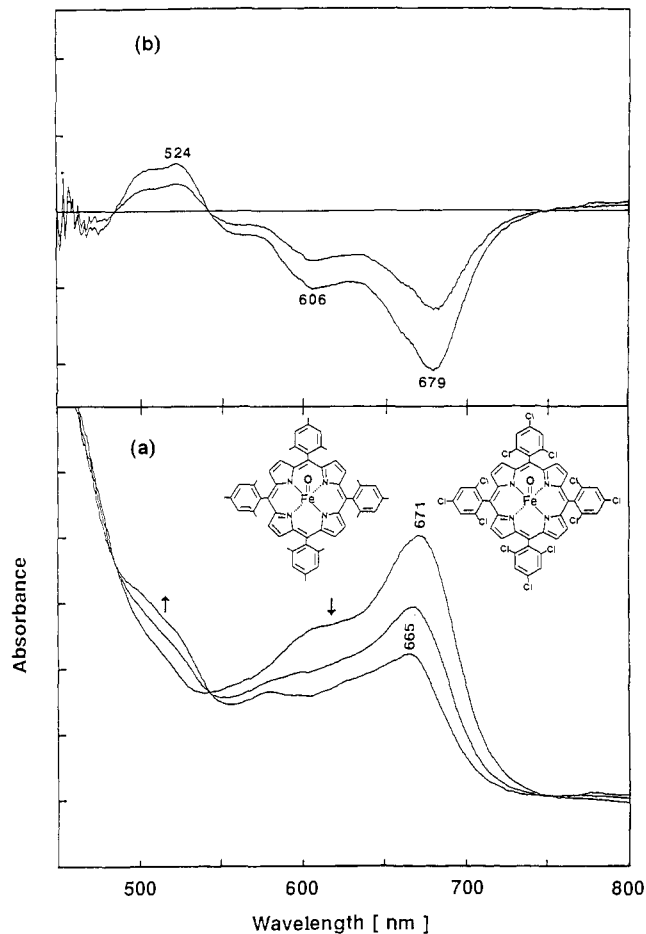


**Figure 7.** (a) Absorption spectral changes of oxoiron(IV) porphyrin  $\pi$ -cation radicals of compounds **5** and **8** for the addition of an excess amount of cyclohexene. (b) Difference absorption spectra on the basis of the initial spectrum.

and iron(III) porphyrin of **4** by comparison with Figure 2. This finding also indicates that only the complex with **4** reacts with cyclohexene. All of these findings indicate that the complex with the higher oxidation potential is more reactive to olefin than that with the lower oxidation potential.

## Discussion

**Electronic State of Oxoiron(IV) Porphyrin  $\pi$ -Cation Radical.** Two types of  $\pi$ -cation radicals have been reported for metalloporphyrins (Figure 9).<sup>18</sup> Large spin density at the bridging meso carbon atom and at the pyrrole nitrogen atom is characteristic of the  $a_{2u}$  radical. The NMR isotropic shift can be related to the  $\pi$ -spin density at the carbon to which the proton is attached.<sup>19</sup> Hence, typical  $a_{2u}$  radicals should give alternate upfield and downfield proton NMR signals for the phenyl ortho, meta, and para protons of **5–8** and large upfield shifts (about 230 ppm) for the meso protons of **1–4** and large upfield shifts (about 230 ppm) for the meso protons of **1–4**. At the other extreme, the  $a_{1u}$  radical has spin density concentrated at the pyrrole carbon atom and has nodes at the meso carbon and the pyrrole nitrogen. Hence, the generation of a typical  $a_{1u}$  radical can be expected to produce a large isotropic shift of pyrrole  $\beta$ -protons of **5–8** and -methyl protons of **1–4** and a small change in the isotropic shift of meso protons (**1–4**) or meso phenyl protons (**5–8**).

The present proton NMR spectra for oxoiron(IV) porphyrin  $\pi$ -cation radicals of **1–4** show large downfield shifts of pyrrole

(18) (a) Dolphin, D.; Felton, R. H. *Acc. Chem. Res.* **1974**, *7*, 26–32. (b) Spaulding, L. D.; Eller, P. G.; Bertrand, J. A.; Felton, R. H. *J. Am. Chem. Soc.* **1974**, *96*, 982–987. (c) Fajer, J.; Borg, D. C.; Forman, A.; Alder, A. D.; Varadi, V. *J. Am. Chem. Soc.* **1974**, *96*, 1238–1239.

(19) Jesson, J. P. *NMR of Paramagnetic Molecules*; La Mar, G. N., Horrocks, W. D., Holm, R. H., Eds.; Academic Press: New York, 1973; pp 1–52.

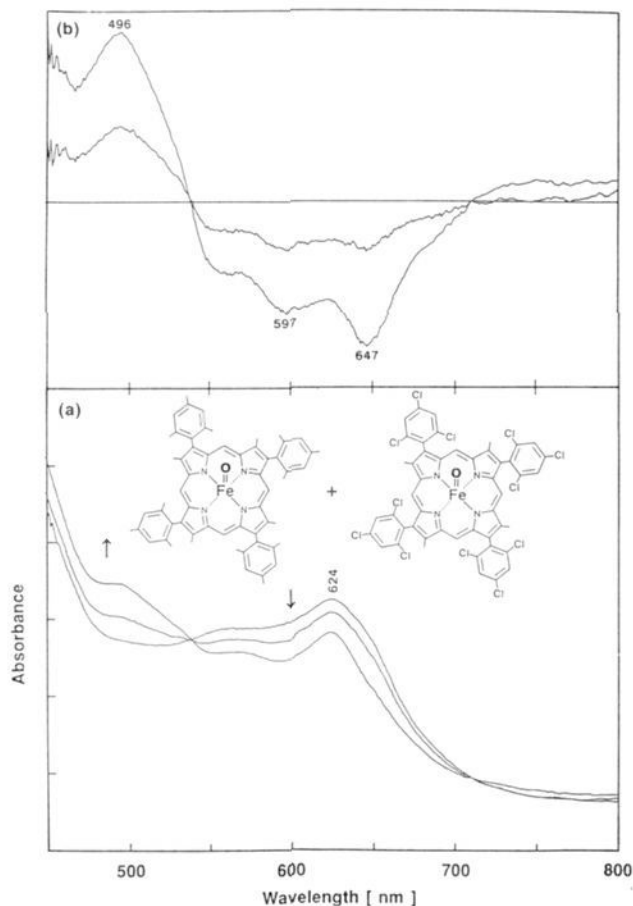


**Figure 8.** (a) Absorption spectral changes of oxoiron(IV) porphyrin  $\pi$ -cation radicals of compounds **1** and **4** for the addition of an excess amount of cyclohexene. (b) Difference absorption spectra on the basis of the initial spectrum.

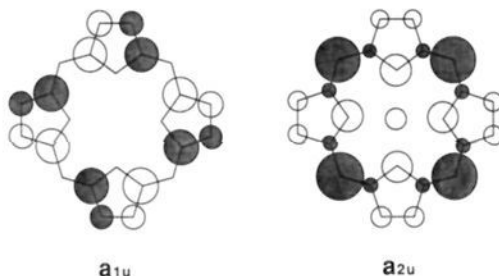


**Figure 9.** Electron spin distribution of porphyrin atomic orbitals. The open circles represent negative signs of the upper lobe of the  $p_x$  AOs.

$\beta$ -methyl protons and small shifts of meso protons, which were attributed to the  $a_{1u}$  radical complexes. On the other hand, the NMR spectra of **5–8** were explained as the generation of a  $a_{2u}$  radical complexes. As shown in Figure 5, the oxoiron(IV) porphyrin  $\pi$ -cation radicals of **5–8** exhibited the large downfield shifts of meta proton signals, which indicates a large spin density on the meso carbon atom. The upfield shifts of pyrrole  $\beta$ -proton signals of oxoiron(IV) porphyrin  $\pi$ -cation radicals of **5–8** were also consistent with the  $a_{2u}$  radical state.

The changes in the NMR spectra with an increase of the electron-withdrawing power of the substituent were interpreted as the mixing of the  $a_{1u}$  and  $a_{2u}$  radical states by vibronic coupling. As shown in Figure 5, the pyrrole  $\beta$ -proton signals for **5–8** exhibited upfield shifts, and the isotropic shifts of the meta proton signal decreased as the electron-withdrawing power of the substituent increased. These spectral changes indicate an increase of spin density at the pyrrole  $\beta$ -carbon and a decrease at the meso

carbon. These spectral changes, therefore, could be reasonably explained if we assume that the  $a_{1u}$  radical state is mixed with the predominant  $a_{2u}$  radical state. Since the temperature dependence of the NMR signals for **5–8** exhibited normal Curie behavior, thermal equilibrium of the  $a_{1u}$  and  $a_{2u}$  states, as observed for ruthenium(II) porphyrin  $\pi$ -cation radicals,<sup>20</sup> was ruled out. A recent Raman study suggested that an important mechanism for  $a_{1u}/a_{2u}$  mixing is the pseudo-Jahn–Teller effect, in which the two states are mixed by a distortion along suitable vibrational modes.<sup>21</sup> The present NMR spectral changes for **5–8** were also consistent with the view that the two radical states are mixed via a pseudo-Jahn–Teller effect.

An electron-withdrawing substituent at the meso position should decrease the energy of the  $a_{2u}$  orbital relative to the  $a_{1u}$  orbital via the interaction of the aryl and porphyrin  $\pi$  orbitals, since electron density is concentrated at the meso carbon atom for the  $a_{2u}$  orbital, while the  $a_{1u}$  orbital has a node at the meso position. This leads to a decrease of the  $a_{1u}$ – $a_{2u}$  energy separation, as shown in Figure 10. Stabilization of HOMOs ( $a_{2u}$  orbital) of **5–8** was supported by the results of electrochemical measurements. Since the orbital mixing depends on the  $a_{1u}$ – $a_{2u}$  energy separation, strong mixing would be expected with an increase in the electron-withdrawing power of the substituent. This is consistent with the present NMR results for **5–8**.

Moreover, a simple explanation can also be offered for the changes of the orbital energy levels of **1–4**. Since the spin density at the pyrrole  $\beta$ -carbon in the  $a_{1u}$  orbital (HOMO for **1–4**) is much smaller than that at the meso carbon in the  $a_{2u}$  orbital (HOMO for **5–8**), the stabilization of the HOMO ( $a_{1u}$  orbital) energy level by pyrrole  $\beta$  substitution (**1–4**) is less significant than that by meso substitution (**5–8**), as suggested by the electrochemical measurements. Since the  $a_{1u}$  and  $a_{2u}$  orbitals have small spin densities at the pyrrole  $\beta$ -carbon, both orbitals are slightly stabilized by an electron-withdrawing substituent, which is indicated by the minor change of the  $a_{1u}$ – $a_{2u}$  energy gap, as shown in Figure 10. Thus, the pyrrole  $\beta$  substituent does not drastically alter the radical orbital occupancy of a meso-unsubstituted oxoiron(IV) porphyrin  $\pi$ -cation radical.

It has been reported that the spectral features of metalloporphyrin  $\pi$ -cation radicals indicate the orbital occupancies.<sup>16,17</sup> The absorption spectra of oxoiron(IV) porphyrin  $\pi$ -cation radicals of **1–4** were similar to that of the  $a_{2u}$  radical complex, while the spectral features of the oxoiron(IV) porphyrin  $\pi$ -cation radicals of **5–8** were characteristic of the  $a_{1u}$  radical complex. However, our NMR data indicated an  $a_{1u}$  radical state for **1–4** and an  $a_{2u}$  radical state for **5–8**, regardless of their visible absorption spectra. This means that the optical spectrum is not a reliable indicator of radical type and that the orbital assignments of compounds **I** of HRP and CAT, based on the spectral absorption features,<sup>17</sup> should be reinvestigated.

Recent resonance Raman spectroscopies<sup>22</sup> of metalloporphyrin  $\pi$ -cation radicals indicate a notable difference in metal–oxo stretching between the  $a_{1u}$  radical complexes and the  $a_{2u}$  radical complexes. They found that the former complexes strengthen the metal–oxo bonds, and the latter complexes weaken, with the formation of the porphyrin  $\pi$ -cation radicals. The resonance Raman study of the present oxoiron(IV) porphyrin  $\pi$ -cation radicals will also give a further insight into this issue.

#### Reactivity of the Oxygen Atom of an Oxoiron(IV) Porphyrin $\pi$ -Cation Radical.

It has been reported that an oxometallopor-

(20) Morishima, I.; Takamuki, Y.; Shiro, Y. *J. Am. Chem. Soc.* **1986**, *25*, 3576–3584.

(21) Czernuszewicz, R. S.; Macor, K. A.; Li, X.-Y.; Kincaid, J. R.; Spiro, T. G. *J. Am. Chem. Soc.* **1989**, *111*, 3860–3869.

(22) (a) Paeng, K.-J.; Kincaid, J. R. *J. Am. Chem. Soc.* **1988**, *110*, 7913–7915. (b) Kincaid, J. R.; Schneider, A. J.; Paeng, K.-J. *J. Am. Chem. Soc.* **1989**, *111*, 735–737. (c) Oliver, Su, Y.; Czernuszewicz, R. S.; Miller, L. A.; Spiro, T. G. *J. Am. Chem. Soc.* **1988**, *110*, 4150–4157.

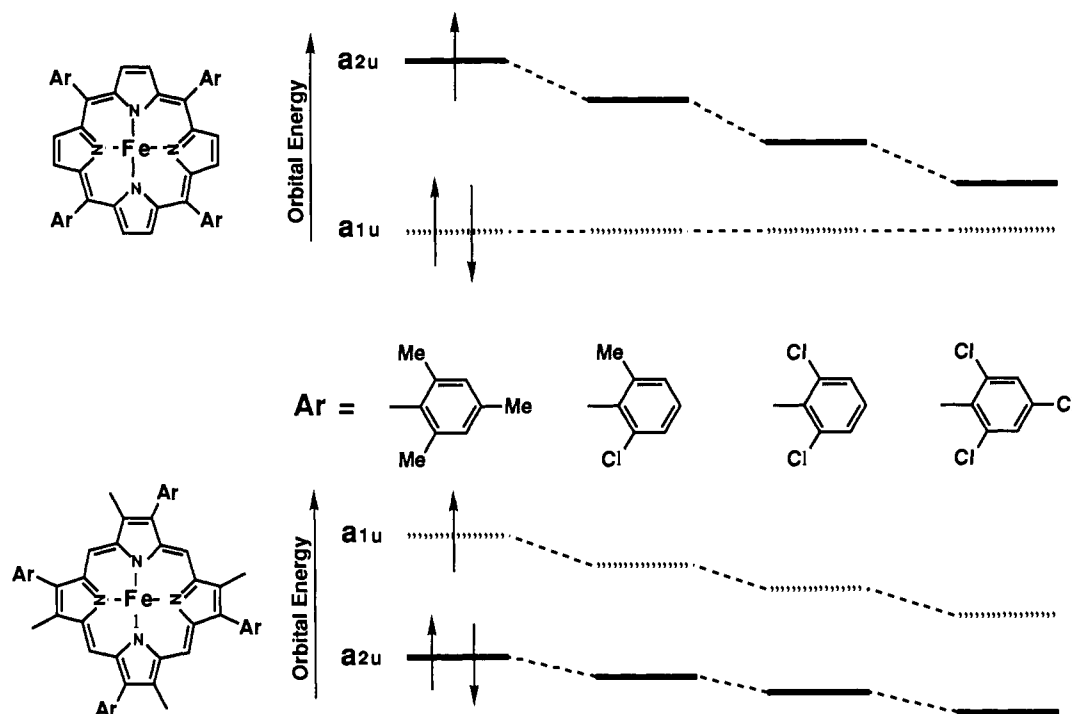


**Figure 10.** Effect of the electron-withdrawing power of substituents on the energy levels of the unperturbed frontier orbitals for oxoiron(IV) porphyrin  $\pi$ -cation radicals of 1–8. The  $a_{1u}$  orbitals for the series of substituents are indicated by dashed lines, and the  $a_{2u}$  orbitals are solid lines.

phyrin complex can oxidize alkenes to epoxides.<sup>23</sup> Although kinetic and mechanistic studies of the epoxidation reaction by metalloporphyrins have been conducted by several groups,<sup>24</sup> the use of oxoiron(IV) porphyrin  $\pi$ -cation radicals for determining the reactivity of the oxygen atom was generally not possible because generation of the oxoiron(IV) porphyrin  $\pi$ -cation radical species is usually a rate-determining step. However, since the present study succeeded in preparing and characterizing various oxoiron(IV) porphyrin  $\pi$ -cation radicals having different radical orbitals and/or oxidation potentials, the comparison of the reactivity of the oxygen atom was determinable.

As discussed in the preceding section, oxoiron(IV) porphyrin  $\pi$ -cation radicals of 1–4 predominantly have the unpaired electron in the  $a_{1u}$  orbital, and those of 5–8 have it in the  $a_{2u}$  orbital. Thus, the competitive reaction of oxoiron(IV) porphyrin  $\pi$ -cation radicals of 1 and 5 with cyclohexene could reveal the effect of the orbital occupancy, since 1 and 5 have almost identical oxidation potentials, as illustrated in Table I. As shown in Figure 6, the absorption spectra showed significant changes with isosbestic points. The clear isosbestic points would be obtained if both complexes react at the same rate, if only one component reacts, or if the equilibrium between these components is rapidly maintained. The equilibrium between the complexes 1 and 5 was ruled out by proton NMR measurements. The broadening of the NMR signals was not observed during the reaction of oxoiron(IV) porphyrin  $\pi$ -cation radicals of 1 and 5 with cyclohexene. Further, recent oxygen and nitrogen transfer studies<sup>25</sup> of metalloporphyrins suggest that the  $\mu$ -oxo dimers are intermediates in the atom transfer reactions. Since the iron porphyrins utilized in the present study are sterically hindered

to inhibit the formation of  $\mu$ -oxo dimer, oxygen transfer between the complexes 1 and 5 does not occur. Thus, although minor deviations from the isosbestic points were observed, the absorption and difference spectra showed that the complexes of 1 and 5 react at the same rate. This means that the reactivity of oxygen atoms of 1 (the  $a_{1u}$  radical complex) and 5 (the  $a_{2u}$  radical complex) is almost the same.<sup>26</sup> This is supported by a recent theoretical calculation involving oxoiron(IV) porphyrin  $\pi$ -cation radicals that showed that the calculated spin densities of the O atom due to delocalization in the Fe–O  $\pi^*$  orbitals are similar for the  $a_{1u}$  and  $a_{2u}$  states.<sup>27</sup>

While the orbital occupancy of the radical has little effect on the reactivity of the oxygen atom, the oxidation potential of the complex has a great effect. As shown in Figures 7 and 8, the absorption spectra for the competitive reactions of two complexes having different oxidation potentials showed clear isosbestic points during the reaction with cyclohexene. Further, the difference spectra showed that only the component with higher oxidation potential reacts with cyclohexene. The increase of the oxidation potential of the iron porphyrin complex activates the oxygen atom of the oxoiron(IV) porphyrin  $\pi$ -cation radical. All of these studies indicated that the reactivity of the oxygen atom of an oxoiron(IV) porphyrin  $\pi$ -cation radical depends on the oxidation potential of the complex, regardless of  $a_{1u}$  and  $a_{2u}$  orbital occupancies.

Several intermediates have been proposed to form in the reactions of high-valent oxoiron porphyrins with alkenes:<sup>28–31</sup>

(23) (a) Groves, J. T.; Nemo, T. E.; Myers, R. S. *J. Am. Chem. Soc.* **1979**, *101*, 1032–1033. (b) Groves, J. T.; Kruper, W. J., Jr. *J. Am. Chem. Soc.* **1979**, *101*, 7613–7615. (c) Creager, S. E.; Murray, R. W. *Inorg. Chem.* **1985**, *24*, 3824–3828. (d) Groves, J. T.; Stern, M. K. *J. Am. Chem. Soc.* **1987**, *109*, 3812–3814. (e) Groves, J. T.; Quinn, R. *J. Am. Chem. Soc.* **1985**, *107*, 5790–5792.

(24) (a) Groves, J. T.; Nemo, T. E. *J. Am. Chem. Soc.* **1983**, *105*, 5786–5791. (b) Traylor, T. G.; Marsters, J. C.; Nakano, T.; Dunlap, B. E. *J. Am. Chem. Soc.* **1985**, *107*, 5537–5539. (c) Dicken, C. M.; Woon, T. C.; Bruce, T. C. *J. Am. Chem. Soc.* **1986**, *108*, 1636–1643. (d) Ostovic, D.; Bruce, T. C. *J. Am. Chem. Soc.* **1988**, *110*, 6906–6908. (e) Traylor, T. G.; Xu, F. F. *J. Am. Chem. Soc.* **1988**, *110*, 1953–1958. (f) Collman, J. P.; Hampton, P. D.; Brauman, J. I. *J. Am. Chem. Soc.* **1990**, *112*, 2977–2986.

(25) (a) Woo, L. K.; Czaplá, D. J.; Goll, J. G. *Inorg. Chem.* **1990**, *29*, 3915–3916. (b) Woo, L. K.; Hays, J. A.; Goll, J. G. *Inorg. Chem.* **1990**, *29*, 3916–3917.

(26) The kinetic studies of the reaction of the individual oxoiron(IV) porphyrin  $\pi$ -cation radicals with cyclohexene indicated that the apparent rate constant of the complex of 5 is about 1.5 times as large as that of 1. A more significant increase in the apparent rate constant was observed in the reaction of the complexes of 7 or 8 with cyclohexene (10–20-fold of that of 5).

(27) Loew, G. H.; Axe, F. U.; Collins, J. R.; Du, P. *Inorg. Chem.* **1991**, *30*, 2291–2294.

(28) Traylor, T. G.; Miksztal, A. R. *J. Am. Chem. Soc.* **1987**, *109*, 2770–2774.

(29) (a) Garrison, J. M.; Bruce, T. C. *J. Am. Chem. Soc.* **1989**, *111*, 191–198. (b) Garrison, J. M.; Ostovic, D.; Bruce, T. C. *J. Am. Chem. Soc.* **1989**, *111*, 4960–4966. (c) Ostovic, D.; Bruce, T. *Acc. Chem. Res.* **1992**, *25*, 314–320.



cation radical, metal-oxo carbon radical, metal-oxo carbocation, and metallaioxetane. From the product analysis of the reaction of the oxoiron(IV) porphyrin  $\pi$ -cation radical of 7 with norbornene, Sawyer et al.<sup>30b</sup> proposed the concerted insertion of an oxygen atom into the  $\pi$ -bond. Several recent studies by Bruice et al.<sup>29</sup> suggest that charge-transfer complex formation is the rate-limiting step and that the complex exhibits a reaction manifold that ranges from concerted to stepwise depending on the nature of the alkene, the iron porphyrin, and the reaction conditions. The present study shows the increase of the reactivity of the oxygen atom with increasing oxidation potential, as was observed for oxochromium(V) porphyrins.<sup>29a</sup> Although this implies a similar reaction mechanism for oxoiron(IV) porphyrin  $\pi$ -cations with olefins, a detailed kinetic study of oxoiron(IV) porphyrin  $\pi$ -cation radicals with alkenes and a study of the effect of the oxidation potential on the electrophilicity of the oxygen atom will be needed to define the mechanism.<sup>32</sup>

**Biochemical Implication.** On the basis of the compound I spectral features, HRP and CAT compounds I are now believed to be low-spin oxoiron(IV) porphyrin  $\pi$ -cation radicals with unpaired electrons in the  $a_{2u}$  and the  $a_{1u}$  orbitals, respectively.<sup>17</sup> This has some implications for the electronic states of HRP and CAT compounds I. The present results for oxoiron(IV) porphyrin  $\pi$ -cation radicals of 1-4 demonstrated that, in  $\beta$ -pyrrole substituted porphyrin, two radical states,  $a_{1u}$  and  $a_{2u}$ , are not switched by the electron-withdrawing power of the substituents and that the radical orbital occupancy of an oxoiron(IV) porphyrin  $\pi$ -cation radical depends on the position of the substituents bound to the porphyrin. It is thus reasonable to expect that HRP compound I possesses the  $a_{1u}$  radical state rather than the  $a_{2u}$  state, because protoporphyrin IX, a prosthetic group of HRP and CAT, is a meso-unsubstituted and pyrrole  $\beta$ -substituted porphyrin. Previously, low-temperature visible spectra of compounds I from HRP reconstituted with 2-formyl-4-vinyldeuteriohemim, 2-vinyl-4-formyldeuteriohemim, 2,4-dimethyldeuteriohemim, and 2,4-diacetyldeuteriohemim showed that these oxoiron(IV) porphyrin

(30) (a) Gold, A.; Doppelt, J. P.; Weiss, R.; Chottard, G.; Bill, E.; Ding, X.; Trautwein, A. X. *J. Am. Chem. Soc.* **1988**, *110*, 5756-5761. (b) Sugimoto, H.; Tung, H.-C.; Sawyer, D. T. *J. Am. Chem. Soc.* **1988**, *110*, 2465-2470.

(31) Collman, J. P.; Kodadek, T.; Raybuck, S. A.; Brauman, J. I.; Papazian, L. M. *J. Am. Chem. Soc.* **1985**, *107*, 4343-4345.

(32) A detailed kinetic study and magnetic property study of oxoiron(IV) porphyrin  $\pi$ -cation radicals are in progress.

$\pi$ -cation radicals assume the  $a_{2u}$  radical state.<sup>7</sup> However, the results of the present study suggest that these compounds I have an  $a_{1u}$  radical state. Although the effect of the protein axial ligand on the electronic state of compound I is not clear, we expect that all compounds I of heme enzymes with meso-unsubstituted iron porphyrin predominantly have an  $a_{1u}$  radical state.

The present study also demonstrated the effect of the radical orbital occupancy and the oxidation potential on the reactivity of the oxygen atom of an oxoiron(IV) porphyrin  $\pi$ -cation radical. Complexes with different oxidation potentials had different effects on the reactivity of the oxygen atom, while those with different radical orbital occupancies did not. It has been thought that the diverse functions of heme enzymes depend on heme environmental structures, such as porphyrin macrocycle structures, the heme proximal ligand, and protein structures in the immediate vicinity of the heme. For example, in spite of a common prosthetic group, the redox potentials of HRP, CAT, and cytochrome P-450 differ because of the differences in the heme proximal ligand; ferric/ferrous couples for P-450, HRP, and CAT are -170, -250, and <-500 mV, respectively.<sup>33</sup> The present results suggest the possibility that the various redox potentials of HRP, CAT, and cytochrome P-450 regulate the reactivities of compounds I. Oxygen transfer reaction by cytochrome P-450 is reasonable for the high oxidation potential of this enzyme. Further, the compound I of chlorin, which is thought to be an intermediate of *Neurospora crassa* catalase,<sup>34</sup> would be less reactive than that of porphyrin since the oxidation potential of iron chlorin is much lower than that of iron porphyrin.

**Acknowledgment.** This work was in part supported by a grant from Nissan Science Foundation. We thank Dr. K. Murakoshi and Professor K. Uosaki for accommodation of electrochemical measurements.

(33) (a) Gunsalus, I. C.; Meeks, J. R.; Lipscomb, J. D.; Debrunner, P.; Münk, E. *Molecular Mechanisms of Oxygen Activation*; Academic Press: New York, 1974; pp 559-613. (b) Yamada, H.; Makino, R.; Yamazaki, I. *Arch. Biochem. Biophys.* **1975**, *169*, 344-353. (c) Williams, R. J. P. *Iron in Biochemistry and Medicine*; Jacobs, A., Worwood, M., Eds.; Academic Press: New York, 1974; pp 183-219.

(34) (a) Jacob, G. S.; Orme-Johnson, W. H. *Biochemistry* **1979**, *18*, 2967-2975. (b) Jacob, G. S.; Orme-Johnson, W. H. *Biochemistry* **1979**, *18*, 2975-2980.